Biochimica et Biophysica Acta, 1153 (1993) 34–42

BBAMEM 76123

Kinetic characterization of Na^+/D-mannose cotransport in dog kidney: comparison with Na^+/D-glucose cotransport

M. Silverman * and L. Ho

Membrane Biology Group, Department of Medicine, University of Toronto, Medical Science Building, Room 7207, Toronto, Ontario M5S 1A8 (Canada)

(Received 2 October 1992)
(Revised manuscript received 28 January 1993)

Key words: Brush-border membrane vesicle; Sodium ion cotransport; D-Mannose cotransport; (Kidney)

Brush-border membrane vesicles (BBMV) prepared from whole dog kidney cortex, or separately from outer cortex (OC) and outer medulla (OM), were used to study the kinetics and inhibition specificity of Na^+-dependent D-mannose cotransport. In BBMV from whole cortex the measured parameters for Na^+/D-mannose uptake were $K_m = 0.07 \pm 0.01$ mM and $V_{max} = 4.19 \pm 0.24$ nmol/mg protein per min ($n = 36$). In OC BBMV the K_m for Na^+/D-mannose was 0.04 mM, $V_{max} = 3.41$ nmol/mg per min. In OM the K_m was 0.06 ± 0.02 mM $V_{max} = 0.18$ nmol/mg per min. Thus only about 5% of Na^+/D-mannose activity occurs in OM. Both mannoheptulose ($K_i = 5.6$ mM) and methyl α-D-mannoside ($K_i = 0.05$ mM) are competitive inhibitors of Na^+/D-mannose uptake, but at comparable concentrations have little effect on Na^+/D-glucose uptake. Phlorizin is a noncompetitive inhibitor of Na^+/D-mannose uptake ($K_i = 4.45$ μM) but a more potent and competitive inhibitor ($K_i = 0.58$ μM) of Na^+/D-glucose uptake. Phloretin ($K_i = 104$ μM) is a noncompetitive inhibitor of Na^+/D-mannose uptake in BBMV. We conclude that Na^+/D-mannose uptake is mediated by a unique high-affinity carrier located in the OC presumably at the luminal surface of the proximal convoluted tubule, with strong specificity requirements for sugars with mannose-like structures (i.e., axial C-2 hydroxyl group). Phlorizin is an inhibitor of both Na^+/D-mannose and Na^+/D-glucose cotransporters but is approx. 10 times less potent for the Na^+/D-mannose system and also has a different mode of inhibition (i.e., noncompetitive vs. competitive). The different phlorizin inhibitory mechanisms on the Na^+/D-glucose and Na^+/D-mannose cotransporters may be mediated by distinct hydrophobic and sugar binding sites that characterize phlorizin–carrier interaction.

Introduction

Early observations in dog kidney using the in vivo multiple indicator dilution technique suggested a luminal transport system for D-mannose independent of that for D-glucose [14]. Subsequent studies in rat and flounder kidney demonstrated that D-mannose transport was Na^+-dependent [3–6,8,11]. More recently, using brush-border membrane vesicles (BBMV) prepared from whole dog kidney cortex [9] it was shown that Na^+ and mannose are cotransported, that the Na^+:D-mannose stoichiometry is 1:1, and that cotransport is electrogenic. Moreover, the sugar specificity characteristics of Na^+/D-mannose transport [9] differ from the Na^+/D-glucose cotransporter. In particular, Na^+/D-mannose uptake is less sensitive to inhibition by the drug phlorizin compared to the potency of this compound in blocking Na^+/D-glucose cotransport. In Ref. 9 we also observed that phlorizin appeared to act as a noncompetitive inhibitor of Na^+-dependent D-mannose uptake, but this finding was not subjected to rigorous kinetic analysis.

The rationale for the present study was to further contrast the functional characteristics of Na^+/D-mannose and Na^+/D-glucose cotransport. This was accomplished by carrying out detailed kinetic inhibition experiments with a variety of compounds including phlorizin, phloretin, mannoheptulose and methyl α-D-mannoside. We believe such information could eventually prove important for several reasons: (i) it will provide useful information for use in a strategy to apply expression cloning techniques for isolation of the cDNA of a Na^+/D-mannose cotransporter, (ii) in the long term our ability to carry out detailed structural-functional comparisons between closely related Na^+-dependent sugar cotransporters (high- and low-affinity glucose carriers, mannose carrier) could prove valuable in localizing sugar and Na^+ binding sites on the individual transporters.

The results of the present study indicate that the Na^+/D-mannose cotransporter is a high-affinity (K_m

* Corresponding author. Fax: +1 (416) 9712132.

approx. 70 μM), low-capacity (V_{max} approx. 4.2 nmol/mg per min) system found almost exclusively in BBMV from outer cortex, thus implying colocalization with the low-affinity (K_m approx. 5 mM) high-capacity (V_{max} approx. 13 nmol/s) Na^+/D-glucose cotransporter presumed to be located at the luminal surface in the pars convoluta [15]. Furthermore, based on substrate specificity, the sugar binding site on the Na^+/D-mannose cotransporter differs significantly from the Na^+/D-glucose carrier. For example both mannoheptulose and methyl α-D-mannoside are potent competitive inhibitors of Na^+/D-mannose uptake with little effect on Na^+/D-glucose cotransport. The K_i for phlorizin inhibition of Na^+/D-mannose cotransport is approx. 10-times larger than its K_i for Na^+/D-glucose cotransport and the inhibition is noncompetitive compared to a competitive mechanism for the Na^+/D-glucose carrier. Also, phlorizin is at least 25-times more potent an inhibitor of Na^+/D-mannnose uptake than is phloretin, the aglycone. The data are consistent with the interpretation that (i) the Na^+/D-mannose cotransporter exists as an independent carrier system at the brush-border membrane of the early region of the proximal convoluted tubule, and (ii) that the mechanism of phlorizin inhibition of both Na^+/D-mannose and Na^+/D-glucose cotransporter is similar and is mediated by drug occupancy of distinct hydrophobic and sugar binding sites on the two carriers.

Materials and Methods

Vesicle preparation

Whole cortical BBM vesicles were prepared from kidneys of mongrel dogs by the $MgCl_2$ precipitation method previously described [9]. Briefly, minced cortical tissue suspended in ice-cold isolation medium (10 mM triethanolamine-HCl, 250 mM sucrose (pH 7.6)) at a concentration of 10 ml/g cortex was homogenized and filtered. Differential centrifugation generated a 'crude membrane fraction' which was then resuspended in Buffer A (10 mM Tris-Hepes, 100 mM mannitol (pH 7.4)) subjected to 10 mM $MgCl_2$ precipitation and low speed centrifugation. The residue supernatant was pelleted at $50\,000 \times g$ to yield the purified brush-border membrane fraction. After vesiculation by sequential passage through 25-G and 30-G needles, the final BBMV fraction was obtained and stored frozen in liquid nitrogen. On the day of the experiment, frozen aliquots of BBMV were incubated at 37°C for 30 min. Unless otherwise noted, they were then suspended either in Buffer A for timed uptake studies or Buffer A 300 (10 mM Tris-Hepes, 300 mM mannitol (pH 7.4)) for initial uptake experiments, and centrifuged at $20\,000 \times g$ for 20 min. The pellet was then resuspended and passed through 25-G and 30-G needles in the same buffer to the required volume at a protein concentration of 1–2 mg/ml.

For preparation of outer cortex and outer medulla, the following procedure was adopted. The bisected kidney was placed in ice-cold heparinized normal saline (0.9%) which helped to intensify the appearance of two distinct regions on the cut surface: a brownish outer region (the cortex) and a pale pinkish red region (the outer medulla). With fine dissecting scissors, the 'outer medullary' tissue (5–7 g/dog) was first carefully dissected out and lifted off the renal column of Bertin in a continuous strip. The 'outer medullary' strip was then carefully trimmed off of surrounding remains of cortical tissue and (whitish rubbery) papillary tissue. The 'outer medulla' was subsequently chopped up into very fine pieces and any white elastic tissue of the minor calyx was carefully removed. Although it was possible to obtain more 'outer medullary' tissue by following the corticomedullary junction and dissecting out the 'sandwiched' pink tissue, this was seldom done because it was too time consuming and might lead to unnecessary proteolysis.

'Outer cortical' tissue (7–10 g/dog) was obtained from the kidney halves after the removal of the 'outer medulla'. The kidney halves were divided into roughly 1-inch squares and fitted onto a Stadie-Riggs microtome. 'Outer cortical' slices of $\simeq$ 0.5–1 mm thick were sectioned out from the kidney surface.

Transport studies

Sugar transport was measured using the Millipore filtration method. As previously documented [9] at 25°C, D-mannose uptake is linear up to 10 s measured over a concentration range 0.01 to 10 mM. Consequently 10-s initial uptake experiments of D-mannose in the presence of a 100 mM NaSCN gradient (outside > inside) were carried out to estimate the initial rate of uptake. Simultaneously measured L-glucose uptake was used to correct for non-specific binding and trapping by filters. D-Mannose binding to membranes was the same in the presence of Na^+ or K^+. Uptake measured in the presence of K^+ rather than Na^+ was taken to be a measure of nonspecific diffusional uptake. Na^+-dependent uptake was calculated by subtracting uptake in the presence of a 100 mM KSCN gradient (outside > inside) from uptake in the presence of a 100 mM NaSCN gradient (outside > inside). All experiments were performed in quadruplicate at 25°C. 50-μl aliquots of suspended vesicles preincubated in appropriate buffer at 25°C was combined with 100 μl of incubation medium containing radiolabelled substrates. After a 10 s incubation, the reaction was terminated by the addition of 1.35 ml of ice-cold stop solution (10 mM Tris-Hepes, 300 mM NaCl, 300 μM phlorizin, 200 mM mannitol) and Millipore filtration (HAWP 0.45 μm) and further washed by 3 × 1.35 ml of

the same solution. The filter was then transferred to Ready Protein (Beckman) and counted. In some experiments to evaluate the effect of various inhibitors on the sugar binding site of either Na^+/D-glucose or Na^+/D-mannose cotransporters, studies were done under Na^+-equilibrium conditions $[Na^+]_o = [Na^+]_i = 100$ mM and $[K^+]_o = [K^+]_i = 25$ mM with the addition of valinomycin at 12.5 μg/mg vesicle protein as a stock solution of 25 mg/ml in ethanol to short circuit the membrane potential gradient. In other experiments, 10-s uptake was measured in the presence of an initial Na^+ gradient (outside > inside), but with a clamped membrane potential [15]. Details of the specific conditions utilized are given in the legends.

Calculations and data analysis

Experimental data (Na^+-dependent) from transport kinetic studies were analyzed by ENZFITTER (Elsevier Biosoft, Cambridge, UK) a sophisticated non-linear regression data analysis program based on the enhanced algorithm of Marquart and a best-fit curve is calculated to the Michaelis-Menten kinetics equation for the mannose carrier generating best-fit values of V_{max} and K_m. The data are weighted either simply, proportionally, or explicitly whichever was deemed most appropriate as well as with robust weighting to eliminate 'outlier'. The fitted data are then transformed into a linear form to the Lineweaver-Burk or Eadie-Hofstee plots. All values quoted are mean ± standard error.

Materials

D-[^{3}H]Mannose (26.9 Ci/mmol), D-[^{3}H]glucose (15.5 Ci/mmol) and L-[^{14}C]glucose (47 mCi/mmol) were purchased from New England Nuclear, Boston, MA. All chemicals used were of the highest purity commercially available. Phlorizin was doubly recrystallized from ethanol. The commercially purchased sugars, mannose, mannoheptulose and methyl α-D-mannoside were checked by thin-layer chromatography and found to contain no significant contaminant of D-glucose.

Results

Na^+/D-mannose cotransport

In an earlier study [9], we provided kinetic evidence that mannose uptake in BBMV occurs by a single high-affinity Na^+-dependent system $K_m = 0.63$ mM and $V_{max} = 3.6$ nmol/mg. Since the present investigation is concerned with detailed analysis of the inhibition kinetics of this system, we felt it was necessary to repeat our original mannose uptake experiments and carry out a more rigorous analysis by fitting the Na^+-dependent D-manose uptake data with a non-linear regression program (ENZFITTER). We compared the adequacy of single- vs. multiple-site kinetic models and determined that only a single-site model gave satisfactory fits to the data. The best fit parameters were $K_m = 0.07 \pm 0.01$ mM, $V_{max} = 4.19 \pm 0.24$ nmol/mg protein per min, $n = 36$.

Localization of Na^+/D-mannose cotransport

Fig. 1 shows Na^+-dependent mannose uptake in BBMV prepared from both outer cortex and outer medulla. The data indicate that Na^+/D-mannose cotransport in OM is only approx. 5% of that found in OC. We conclude that this minor activity must be due to a small contaminant of OC nephron segments in the OM preparation. This finding colocalizes the Na^+/D-mannose cotransport system to the same region as the low-affinity Na^+/D-glucose carrier, presumably the apical surface of the pars convoluta [15]. It is worth emphasizing that in outer cortex the Na^+/D-mannose cotransporter is a high-affinity system with a K_m approx. 100-times lower than the Na^+/D-glucose cotransporter, but it is a comparatively low capacity system with a V_{max} of only approx. 25% of that of the Na^+/D-glucose carrier.

Mannoheptulose

As shown in Fig. 2, mannoheptulose is a seven carbon sugar which retains a strong structural similarity to D-mannose. It is not surprising therefore, that in

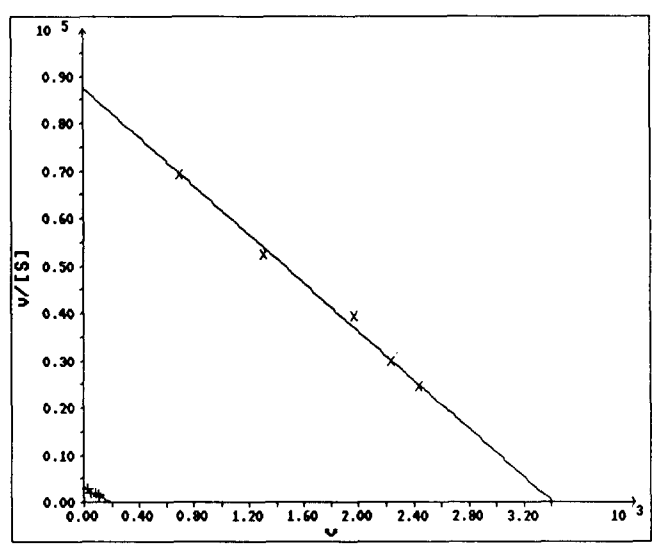

Fig. 1. Na^+-dependent D-mannose flux into outer cortical (×) and outer medullary (+) BBMV as shown in an Eadie-hofstee plot. The data points are from a typical experiment as described in Materials and Methods. Vesicles were preincubated in Buffer A300. Incubation medium was Buffer A with 100 mM NaSCN or 100 mM KSCN (final concentration) and D-mannose over a concentration range of 0.01–0.1 mM. Uptake was measured after 10 s of incubation at 25°C. A non-linear regression analysis curve fit yields $K_m = 0.04$ mM $V_{max} = 3.4 \pm 0.08$ nmol/mg protein per min for outer cortex and $K_m = 0.06 \pm 0.02$ mM, $V_{max} = 0.19 \pm 0.02$ nmol/mg protein per min for outer medulla.

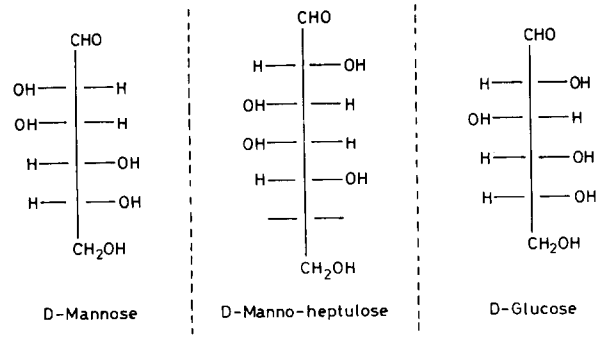

Fig. 2. Fisher projections illustrating the structural similarity of D-mannose and D-mannoheptulose. For comparison the structure of D-glucose is also shown.

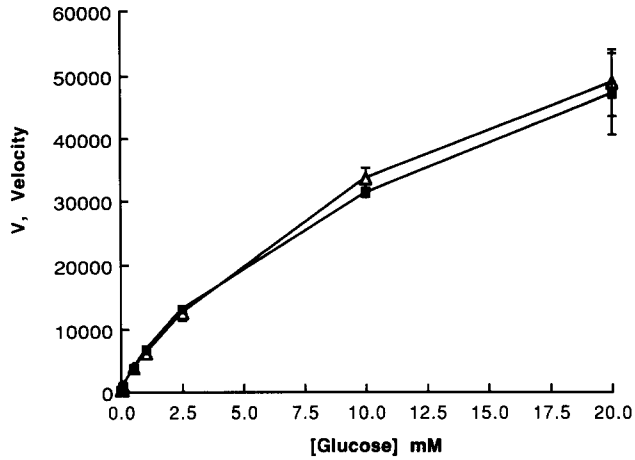

Fig. 4. Effect of mannoheptulose on D-glucose uptake under Na^+ equilibrium conditions and in the absence of a membrane potential. The data points are from a typical experiment. Vesicles were divided into three sets. Two sets were prepared in Buffer A containing 100 mM NaCl and 25 mM KCl with the addition of valinomycin (see Methods). The incubation medium contained 100 mM NaCl and 25 mM KCl plus D-glucose at concentrations over the range 0.025 to 20 mM in the presence or absence of mannoheptulose. The third set was prepared in Buffer A containing 125 mM KCl and valinomycin. The incubation medium contained 125 mM KCl and D-glucose in concentrations ranging from 0.025 to 20 mM. The data plotted represent Na^+-dependent D-glucose uptake in the absence of mannoheptulose (△) and with 15 mM mannoheptulose (■) given as v, velocity (nmol/min per mg protein).

our earlier study we found mannoheptulose to be an effective inhibitor of Na^+/D-mannose uptake into BBMV [9]. To clarify the nature of this inhibition, we examined in more detail the inhibition kinetics of mannoheptulose at 0, 6, and 12 mM concentrations on the Na^+-dependent component of D-mannose initial uptake (0.01 → 0.1 mM). The results are shown in Fig. 3 in the form of Lineweaver-Burk and Eadie-Hofstee transformations. The data indicate that mannoheptulose is a competitive inhibitor of the Na^+/D-mannose cotransporter, with a mean K_i of 5.61 ± 0.05 mM ($n = 2$). The data in Fig. 3 were obtained in the presence of a Na^+ gradient (outside > inside) and negative inside membrane potential. In the absence of Na^+ gradient and membrane electrical potential driving forces, Na^+/D-mannose uptake is very low and the results are quantitatively unreliable. Nevertheless several experiments were attempted under these conditions and results qualitatively identical to those shown in Fig. 4 were obtained (data not shown).

In contrast to the data in Fig. 3, mannoheptulose under equilibrium conditions up to 15 mM has no significant inhibitory effect on Na^+-dependent D-glu-

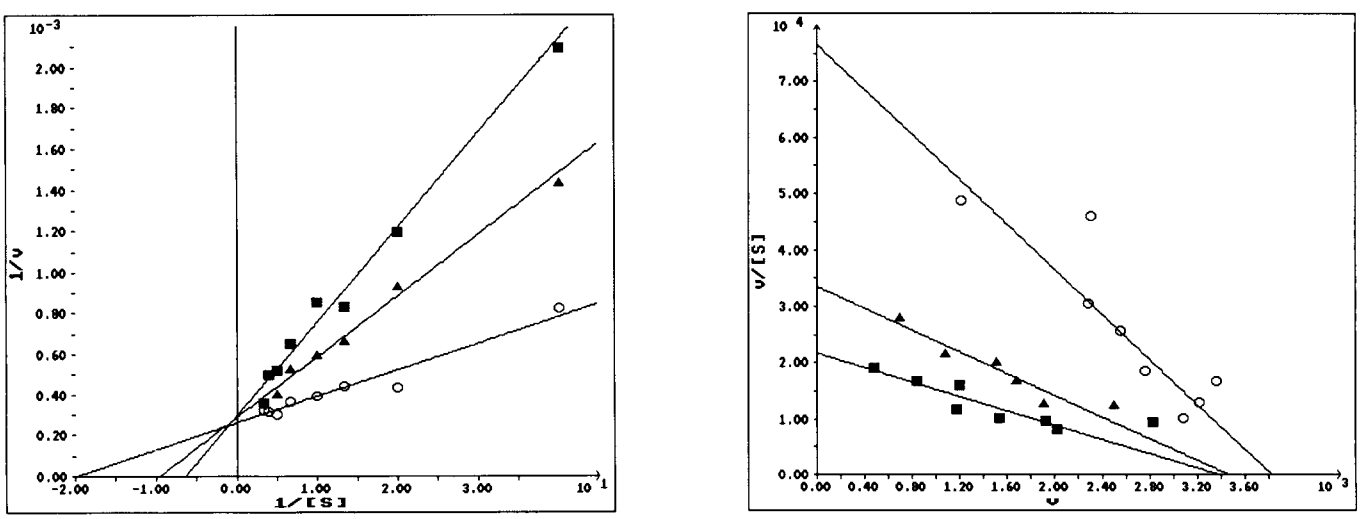

Fig. 3. Inhibition kinetics of mannoheptulose on the Na^+-dependent D-mannose initial uptake. The data points are from a typical experiment. BBM vesicles were suspended in Buffer A300. The incubation medium was Buffer A with either 150 mM NaSCN or 150 mM KSCN and D-mannose over a concentration range of 0.01–0.1 mM. Na^+-dependent component of initial uptake was obtained by subtracting the uptake at each concentration in the absence of Na from that found in its presence and in the absence (○) or in the presence of 6 mM (▲) or 12 mM (■) mannoheptulose. The transformation to (A) a Lineweaver-Burk plot and (B) an Eadie-Hofstee plot were done with the ENZFITTER program.

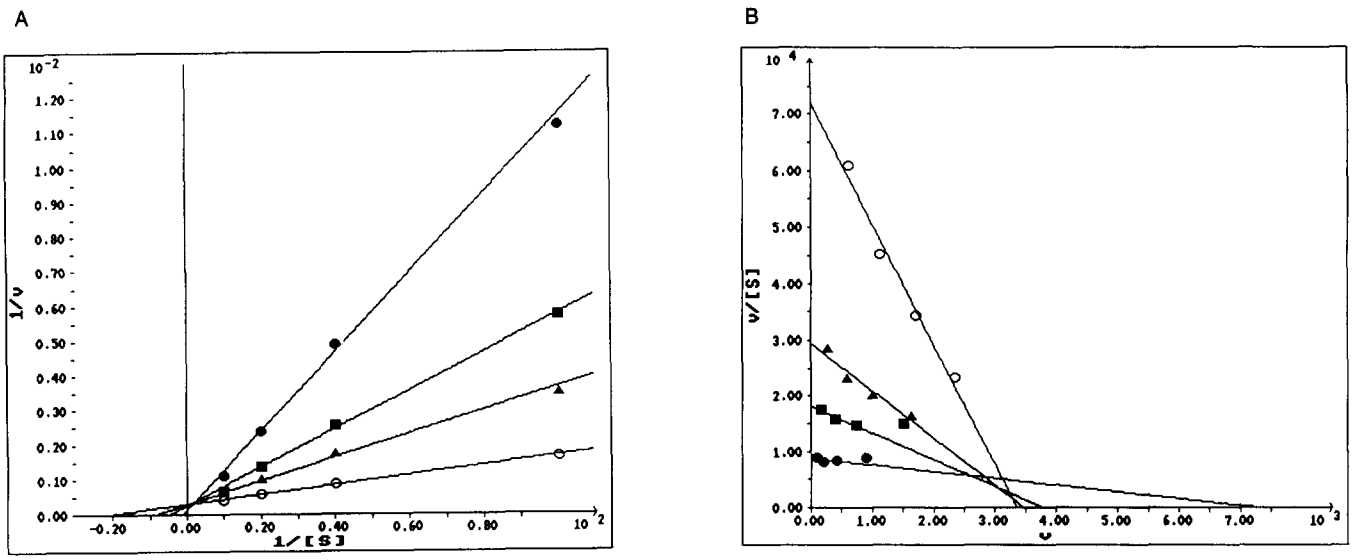

Fig. 5. Inhibition kinetics of methyl α-D-mannoside on the NA^+-dependent initial uptake of D-mannose. Vesicles were prepared in Buffer A300. Incubation medium was Buffer A with either 150 mM NaSCN or 150 mM KSCN and a D-mannose concentration ranging from 0.01 to 0.1 mM. The inhibitory effect of methyl α-D-mannoside was studied at various concentrations starting from 0 mM (○), 0.05 mM (△), 0.1 mM (■) to 0.25 mM (○). The Na^+-dependent component of initial (10-s) uptake was calculated by subtracting the Na^+-independent component from the (total) D-mannose uptake. The transformations to (A) a Lineweaver-Burk plot and (B) an Eadie-Hofstee plot were done utilizing the ENZFITTER program. A non-linear regression analysis fit yields K_m for the Na^+/D-mannose cotransporter of 0.05 and a K_i for methyl α-D-mannoside of 0.05 ± 0.02 ($n = 11$).

cose initial uptake measured over the concentration range 0.025–20 mM (Fig. 4). We conclude therefore that sugar binding sites on the Na^+-dependent D-mannose and Na^+-dependent D-glucose cotransporters are quite different from each other.

Methyl α-D-mannoside

When methyl α-D-mannoside was tested as an inhibitor of both Na^+/D-mannose and Na^+/D-glucose cotransport, no effect was observed on Na^+/D-glucose uptake up to concentrations of 1.0 mM (data not shown). But methyl α-D-mannoside proved to be a very effective inhibitor of Na^+/D-mannose uptake, exhibiting competitive kinetics with a K_i of approx. 49 μM (Fig. 5). Since the K_i for methyl α-D-mannoside is almost the same as the K_m for Na^+/D-mannose cotransport, the affinity of mannose and methyl α-D-mannoside for the Na^+/D-mannose cotransporter must be very similar. This is analogous to the competitive inhibition observed between D-glucose and methyl α-D-glucoside for the Na^+/D-glucose carrier [17]. We conclude that for both Na^+/D-mannose and Na^+/D-glucose cotransporters in OC, substitution of a bulky methyl group at the alpha anomeric position has almost no effect on pyranoside-cotransporter interaction.

Phlorizin

Phlorizin has long been recognized as a potent competitive inhibitor of Na^+-dependent D-glucose, in particular of the low-affinity system in the early proximal tubule, where the K_i of phlorizin inhibition has been determined to be in the approx. 0.5 μM range [16,17]. There is also considerable evidence that phlorizin binds to, but does not enter BBM vesicles [18]. In our earlier

TABLE I

Effect of phlorizin on Na^+/D-mannose cotransport

A summary of inhibition kinetics of phlorizin on the initial (10-s) uptake of D-mannose into BBM vesicles. Uptake studies were done under a Na^+ gradient of 100 mM and a negative membrane potential. The mannose concentration range was 0.01–0.05 mM. The Michaelis constants V_{max} and K_m were generated by a non-linear regression curve fit of the data to the Michaelis-Menten kinetic equation. The apparent K_i for phlorizin was derived from the equation $V'_{max} = V_{max}/(1 + ([I]/K_i))$. The values quoted are the means ± S.E.

Phlorizin (μM)	0	5	10	25	50	100
V_{max} (nmol/mg protein per min)	4.8 ±0.5	3.5 ±1.0	2.6	2.2±0.3	1.7 ±0.8	1.3 ±0.9
K_m (mM)	0.08±0.02	0.06±0.01	0.05	0.1±0.04	0.12±0.08	0.07±0.03

Phlorizin $K_i = 14.8 \pm 1.9$ μM $n = 14$

study [9] we demonstrated that phlorizin was an effective inhibitor of Na^+-dependent mannose uptake, and a preliminary review of the data suggested that the mechanism of inhibition might be noncompetitive. This was unexpected (i.e., we expected higher K_i than for Na^+/D-glucose carrier but still a competitive mechanism). If phlorizin was indeed acting as a non competitive inhibitor of the Na^+/D-mannose carrier this would be an extremely interesting result because the usual mechanism for non competitive inhibition of transport is through binding of inhibitor to the cytoplasmic face of the carrier and yet all published evidence [12] suggests that phlorizin does not penetrate to the inside of the membrane vesicle. The problem with the studies in Ref. 9 is that only a limited number of inhibitor concentrations were assessed, and the kinetic analysis was not sufficiently rigorous to draw definitive conclusions about the nature of phlorizin inhibition. Therefore we systematically repeated these experiments. Table I is a summary of the kinetic parameters determined after non-linear regression fitting. It is apparent that the K_m remains unaffected, but the V_{max} is reduced in a dose dependent manner, indicating a noncompetitive mode of inhibition. When displayed on a Hane's plot (data not shown) parallel lines were obtained consistent with noncompetitive rather than uncompetitive inhibition kinetics. The mean phlorizin K_i is approx. 15 μM, significantly less than the K_m for D-mannose (approx. 73 μM). These results indicate that although phlorizin is a noncompetitve inhibitor of Na^+/D-mannose cotransport but a competitive inhibitor of Na^+/D-glucose cotransport, in both instances phlorizin has greater affinity to the cotransporter than does the natural sugar substrate.

Equilibrium binding for phlorizin in BBMV preparations requires 3–5 min [12]. Although after 10 s, phlorizin is obviously an effective inhibitor of Na^+/D-mannose and also of Na^+/D-glucose cotransport [17], we were still concerned that the apparent noncompetitive inhibitory action of phlorizin on mannose might be 'artifactual' in the sense that the inhibition measurements were carried out before maximal equilibrium binding of phlorizin had been achieved. Therefore we reexamined phlorizin inhibition of Na^+-dependent D-mannose transport using a protocol which allowed for preequilibration of BBMV with phlorizin to achieve maximal equilibrium binding (Fig. 6, see legend for details). Inspection of Fig. 6 shows that phlorizin inhibition kinetics remain noncompetitive. But the K_i for phlorizin decreased from approx. 15 to approx. 4 μM following preequilibration presumably because this protocol allowed for maximal drug occupancy. Thus phlorizin is a more effective inhibitor of Na^+/D-glucose transport in outer cortex (K_i is approx. 1:10) than of Na^+/D-mannose transport; but the mechanism of inhibition is different: competitive for the Na^+/glucose carrier and noncompetitive for the Na^+/mannose system.

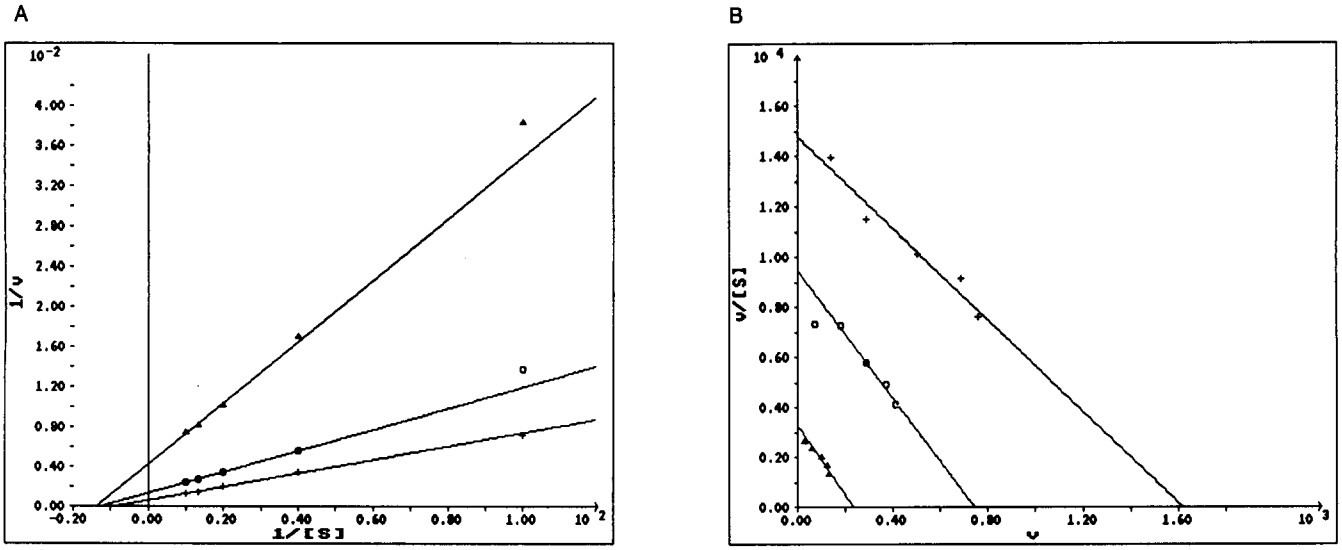

Fig. 6. Effect of phlorizin on the kinetics of initial (10-s) Na^+-dependent D-mannose uptake using a phlorizin preincubation protocol to achieve inhibition equilibrium binding conditions. The data points are from a typical experiment. The data are displayed as (A) Lineweaver-Burk plot and (B) Eadie-Hofstee plot. Aliquots of BBMV were preincubated for 30 min in Buffer A containing valinomycin (12.5 μg/mg vesicle protein) with 40 mM NaCl and 25 mM KCl or Buffer A containing 25 mM KCl. The preincubation buffer for both types of BBMV also contained zero (+), 7.5 μM (○) or 15 μM (△) concentration of phlorizin. After the preequilibration procedure was over, D-mannose uptake was measured at 10 s following addition of an incubation medium containing Buffer A, D-[^{3}H]mannose and L-[^{14}C]glucose (0.01–0.1 mM) phlorizin (0, 7.5 μM, 15 μM) and with 140 mM NaCl and 25 mM KCl or Buffer A and 25 mM KCl. The Na^+-dependent component of mannose initial uptake was obtained by subtracting values measured in the presence of K^+ from uptakes measured with Na^+ at corresponding phlorizin concentration. Apparent K_i for phlorizin is 4.45 μM.

TABLE II

Effect of phloretin on Na^+/D-mannose cotransport

Summary table of phloretin inhibition on D-mannose initial uptake. The experimental conditions were similar to that given in the legend of Table I. Mannose concentration range was 0.01–0.64 mM. The apparent K_i for phloretin was calculated from the equation $V'_{max} = V_{max}/(1+([I]/K_i))$. The values quoted are the means ± S.E.

Phloretin (μM)	0	50	100	200
V_{max} (nmol/mg protein per min)	4.2 ±0.9	2.3 ±0.1	1.6 ±0.01	1.2 ±0.2
K_m (mM)	0.08±0.03	0.07±0.03	0.07±0.03	0.06±0.04

Phloretin $K_i = 104 \pm 14$ μM $n = 7$

Phloretin

Because of the very significant differences observed in the specificity of sugar substrate interaction with the Na^+/D-mannose and Na^+/D-glucose cotransporters, we reasoned that the pyranoside moiety of phlorizin was participating to a negligible degree in the inhibition activity of the drug and consequently that phloretin, the aglycone of phlorizin should inhibit Na^+/D-mannose cotransport to the same degree as phlorizin. As shown in Fig. 7, phloretin, similar to phlorizin, exhibits noncompetitive inhibition of Na^+/D-mannose uptake. The kinetic parameters are summarized in Table II. The K_i for phloretin was found to be approx. 100 μM, i.e., 5–10-times higher than the K_i for phlorizin and about 50% higher than the K_m for D-mannose. We conclude that although phloretin probably inhibits Na^+/D-mannose cotransport by binding to a specific hydrophobic domain on the nontransported form of the carrier overall phloretin is a much less effective inhibitor of this system than is phlorizin.

Discussion

The results reported here confirm the existence of a unique Na^+/D-mannose cotransporter in dog kidney and localize this carrier to the outer cortex brush-border membrane presumably at the level of the proximal convoluted tubule – in the same location as postulated for the putative low-affinity Na^+/D-glucose carrier. However, the Na^+/D-mannose cotransporter is a relatively high-affinity low-capacity system compared to the cortical Na^+/D-glucose carrier which exhibits characteristic low-affinity high-capacity transport kinetics. Both Na^+/D-mannose and Na^+/D-glucose cotransporters show Na^+:pyranoside stoichiometry [9,17].

It is worth commenting on the substrate specificity of the Na^+/D-mannose carrier compared to the Na^+/D-glucose carrier. The data in the present study indicate the strong preference of the Na^+/D-mannose cotransporter for substrates with 'mannose-like' structural characteristics (i.e., *axial* OH at C-2 position of pyranoside), e.g., mannoheptulose and methyl α-D-mannoside. This behavior is entirely consistent with earlier investigations of the sugar specificity characteristics of the Na^+/D-glucose carrier [13] in which a strong requirement for an *equatorial* OH at the C-2 position was documented.

As stated in the Introduction, the results of the present study in defining the in situ kinetics and specificity characteristics of the renal Na^+/D-mannose co-

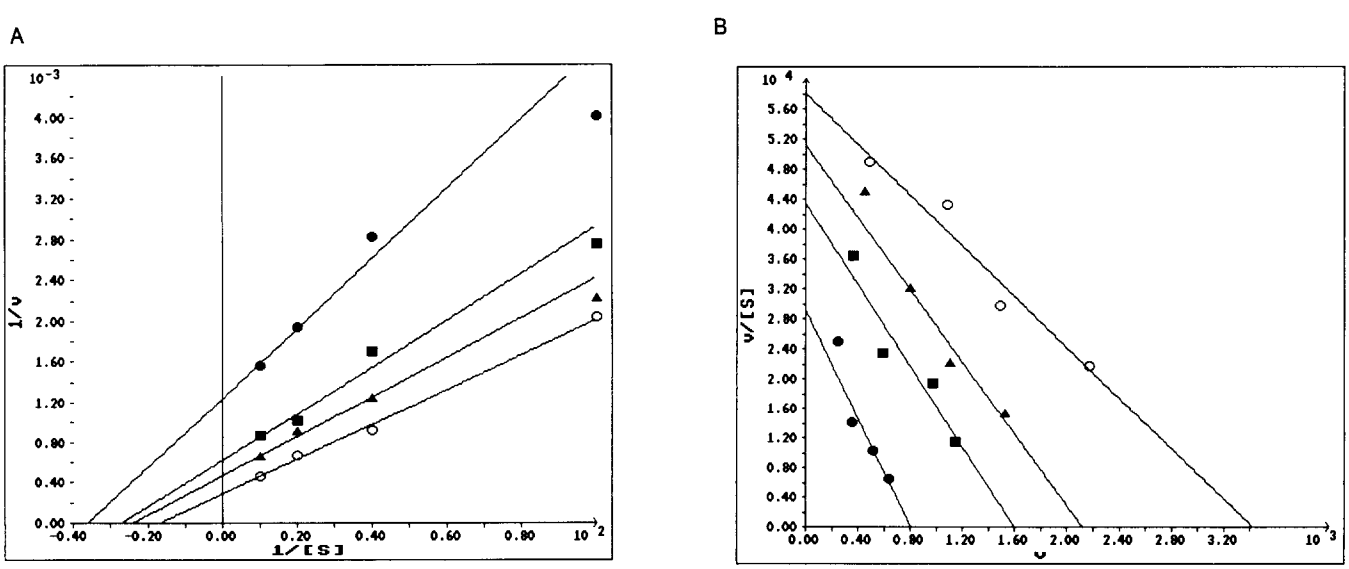

Fig. 7. Inhibitory effect of phloretin on the D-mannose transporter under Na^+-gradient conditions. The data points are from a typical experiment. BBMV were prepared in Buffer A300. Incubation medium was Buffer A with either 150 mM NaSCN or 150 mM KSCN and a D-mannose concentration range of 0.01–0.1 mM. The Na^+-dependent component of D-mannose initial uptake was obtained by subtracting the uptake values measured in the absence of Na from uptake in the presence of Na^+ under different phloretin inhibition concentrations (○), 0.05 mM (▲), 0.1 mM (□) or 0.2 mM (●). The data are displayed as (A) a Lineweaver-Burk and (B) an Eadie-Hofstee plot.

transporter and its comparison with the renal Na^+/D-glucose cotransporter will be helpful over the long term in characterizing the nature of the sugar binding sites on the family of Na^+-dependent cotransporters.

In exploring the question of inhibition specificity of the Na^+-mannose cotransporter we also came upon some unexpected findings in relation to the mechanism of phlorizin action. The mechanism of phlorizin inhibition of the Na^+/D-glucose carrier in the outer cortex is quite different from its inhibitory action on the Na^+/D-mannose carrier. The K_i of phlorizin inhibition of the Na^+/D-glucose cotransporter is approx. 1000-times less than the K_m for D-glucose. The accepted explanation [1,2] is that the phloretin moiety of phlorizin binds to a hydrophobic region of the cotransporter, leading to a conformational change that favours the binding of the glycoside moiety on phlorizin to the sugar binding site. This is easily understood because the sugar binding site on the Na^+/D-glucose carrier strongly favours pyranosides which are 'glucose' like. But for the Na^+/D-mannose carrier, given the strong preference for binding of 'mannose'-like pyranosides, the relatively strong inhibitory activity (with a K_i approx. 1:4 of the D-mannose K_m) was not expected.

Our first thought was that phlorizin inhibits Na^+/D-mannose cotransport, not because of any specific interaction with the sugar binding site, but through occupancy of a functionally coupled hydrophobic protein domain. Indeed there is evidence (at least for the Na^+/D-glucose cotransporter) that phloretin competitively inhibits Na^+-dependent phlorizin binding to this hydrophobic region [7]. But if this were the case, the aglycone phloretin should be just as effective an inhibitor of Na^+/D-mannose uptake as is phlorizin. The data show the opposite, i.e., the K_i for phloretin inhibition of Na^+/D-mannose cotransport is about 5–10-times greater than the K_i for phlorizin. This means that the pyranoside moiety on phlorizin must participate in the drug–carrier interaction. The most reasonable interpretation is that through its hydrophobic interaction with the carrier, phlorizin brings about a conformational change of the sugar binding site on the mannose carrier, which then allows the D-glucose pyranoside moiety on phlorizin to be more readily bound, even though the 'fit' is not optimal.

We speculate therefore that phlorizin inhibits both Na^+/D-glucose and Na^+/D-mannose carriers through a very similar mechanism – (i) highly specific binding to a hydrophobic domain of both carriers, which (ii) then induces a conformational change in the cotransporter allowing the glucose-like pyranoside on phlorizin to 'dock' in the sugar binding site.

For the case of the Na^+/D-glucose carrier the consequence of this sequential two site phlorizin binding is that the affinity of drug-transporter binding is enhanced approx. 1000 compared to the affinity of D-glucose which occupies only one site. But glucose competitively inhibits phlorizin binding because glucose is able to displace the pyranoside moiety of phlorizin (in the presence of Na^+) resulting in a conformational change [10] that reduces the affinity of phlorizin for its hydrophobic binding site.

When phlorizin interacts with Na^+/D-mannose carrier we postulate a similar sequence of molecular events, i.e., first phlorizin binds to a hydrophobic site leading to a conformational change that favours occupancy of the sugar binding site. But in this case, the phlorizin pyranoside (glucose) moiety 'fit' with the mannose preferring sugar binding site, must cause sufficient distortion locally so that it becomes energetically unfavourable for a free mannose molecule to displace the glucose moiety on phlorizin. Consequently the drug (phlorizin) remains bound to the nontransported carrier, anchored via its hydrophobic interaction, yielding noncompetitive inhibition kinetics.

There is nothing in the present study to contradict earlier work which suggested that the *high-affinity* Na^+-phlorizin receptor is identical to or part of the outer cortical or outer medullary (or both) Na^+/D-glucose cotransporters. The possibility that there is a low-affinity Na^+-dependent phlorizin receptor corresponding to the Na^+/D-mannose cotransporter has not been excluded. It is also possible that Na^+ is not even necessary for phlorizin inhibition of Na^+/D-mannose cotransport. In this context it is worth recalling that when phlorizin binding is carried out over a wider concentration range in the *absence* of Na^+, a low-affinity site of approx. 10 μM K_i is observed [18]. But it is not known if this low-affinity phlorizin binding site is affected by D-mannose.

In the present study we have compared two similar but almost certainly different Na^+-cotransport systems from the dog outer kidney cortical region: the Na^+/D-glucose cotransporter and the Na^+/D-mannose cotransporter. It is perhaps not surprising that the drug phlorizin inhibits both, likely through binding to a similar hydrophobic protein domain on both carriers. In future experiments it will be of interest to map out this hydrophobic binding site, since it may play a pivotal role in controlling not only sugar binding but also the translocation process.

Acknowledgement

This work was supported by a grant from the Medical Research Council of Canada to the Membrane Biology Group.

References

1 Alvarado, F. (1967) Biochim. Biophys. Acta 135, 483–495.
2 Diedrich, D.F. (1963) Biochim. Biophys. Acta 71, 688–700.

3 Kleinzeller, A. (1970) Biochim. Biophys. Acta 211, 264–276.
4 Kleinzeller, A., Kolinska, J. and Benes, I. (1967) Biochem. J. 104, 852–860.
5 Kleinzeller, A., McAvoy, E.M. and McKibbin, R.D. (1980) Biochim. Biophys. Acta 600, 513–529.
6 Kleinzeller, A., Tam, I., Kanter, R.K. and McAvoy, E.M. (1974) Biochim. Biophys. Acta 373, 397–403.
7 Koepsell, H., Fritzsch, G., Korn, K. and Madrala, A. (1990) J. Membr. Biol. 114, 113–132.
8 McNamara, P.D., Rea, C., Ozegovic, B. and Segal, S. (1976) Am. J. Physiol. 231, 9–13.
9 Mendelssohn, D.C. and Silverman, M. (1989) Am. J. Physiol. 257 (Renal Fluid Electrolyte Physiol. 26), F1100–F1107.
10 Peerce, B.E. (1990) J. Biol. Chem. 265, 1737–1741.
11 Pritchard, J.B., Booz, G.W. and Kleinzeller, A. (1982) Am. J. Physiol. 242 (Renal Fluid Electrolyte Physiol. 11), F412–F422.
12 Silverman, M. and Black, J. (1975) Biochim. Biophys. Acta 394, 10–30.
13 Silverman, M. and Turner, R.J. (1992) in Handbook of Physiology, Section 8, Renal Physiology (Windhager, E.E., ed.), Vol. 11, Chapter 43, pp. 2017–2038, Oxford.
14 Silverman, M., Aganon, M.A. and Chinard, F.P. (1970) Am. J. Physiol. 218, 743–750.
15 Turner, R.J. and Moran, A. (1982) Am. J. Physiol. 242 (Renal Fluid Electrolyte Physiol. 11), F406–F414.
16 Turner, R.J. and Moran, A. (1982) J. Membr. Biol. 67, 73–80.
17 Turner, R.J. and Silverman, M. (1978) Biochim. Biophys. Acta 511, 470–486.
18 Turner, R.J. and Silverman, M. (1981) J. Membr. Biol. 58, 43–55.